Laser and Particle Beams (2017), *35*, 391–396.

doi:10.1017/S0263034617000325

Distribution and formation of particles produced by laser ablation of cyclotetramethylene tetranitramine

W. ZHANG, R. SHEN, Y. YE, L. WU, P. ZHU, AND Y. HU

Department of Applied Chemistry, School of Chemical Engineering, Nanjing University of Science and Technology, Nanjing, People's Republic of China

(RECEIVED 4 March 2017; ACCEPTED 12 May 2017)

Abstract

An experimental investigation into laser ablation of secondary explosives, cyclotetramethylene tetranitramine (HMX), has been carried out by using a solid-state laser at the wavelength of 1064 nm. The ion particles of decomposition were detected by using a time-of-flight mass spectrometer. Possible attributions of both negative ions and positive ions were obtained. Some obvious peaks were found at $m/z = 18$, 28, 46, 60, and 106, corresponding to H_2O, $CO/N_2/H_2CN$, NO_2, CH_2NO_2/N_2O_2, and $N(NO_2)_2/CH_2(NO_2)_2$, respectively. According to the distribution of the particles, three possible pathways were proposed to explain the process of particles. The results may shed some light on the possible decomposition mechanism of HMX under laser initiation.

Keywords: Cyclotetramethylene tetranitramine; Decomposition mechanism; Laser initiation; Particles distribution

1. INTRODUCTION

Compared with the traditional mechanical initiation or electric initiation, laser initiation of explosives has the characteristics of high safety and high reliability (Myers *et al*., 2016). In the past decades, research on laser initiation of energetic materials has been carried out world widely, including experimental (Ahmad *et al*., 2009; Aluker *et al*., 2010; Damm & Maiorov, 2010; Abdulazeem *et al*., 2011; Zhang *et al*., 2014, 2015) and theoretical studies (Babushok *et al*., 2007; Cohen *et al*., 2007; Lee *et al*., 2008; Civiš *et al*., 2011; Aluker *et al*., 2012). Up to present, there were two explanations for the mechanism of laser initiation: Thermochemical mechanism (Bourne, 2001; Shui *et al*., 2013), and photochemical mechanism (Kuklja *et al*., 2001; Kuklja, 2003; Bhattacharya *et al*., 2010, 2012; Aluker *et al*., 2011).

Cyclotetramethylene tetranitramine (HMX) is a powerful and relatively insensitive nitroamine high explosive, which is commonly used in military (Pravica *et al*., 2010; Sharia *et al*., 2013). Typical structure of HMX is shown in Figure 1.

A few number of studies were conducted to establish the numerical model of laser initiation of HMX (Dik *et al*., 1991; Meredith *et al*., 2015). CO_2 laser ignition experiments of HMX were performed by Ali *et al*. (2003) to illustrate the reactive mechanism during deflagration-to-detonation transitions. Laser-assisted combustion of HMX at heat fluxes of 100 and 300 W/cm^2 was investigated, the flame and surface structures were observed by using a high-magnification video system, the major species at the surface were H_2O, CH_2O, HCN, NO_2, N_2O, N_2, CO, and NO (Tang *et al*., 1999). Greenfield employed femtosecond laser pump–probe experiments at three wavelengths (226, 228, and 230 nm) to investigate the mechanisms and dynamics of the photodissociation of HMX, the results indicated that the decomposition dynamics of HMX was in the time scale of the femtosecond laser pulse duration (180 fs) (Greenfield *et al*., 2006). Sunku *et al*. (2013) reported laser induced breakdown spectroscopy spectra of HMX by using ns and fs pulses, C, CN peaks, and other atomic peaks were recorded.

Fundamental understanding of mechanisms of interaction between laser beam and materials is far from complete (Yazdani *et al*., 2009), and ways to control chemical reactions in energetic materials with laser excitation are yet to be established (Aluker *et al*., 2012; Wang *et al*., 2017). To gain a better understanding of the various reactive transient species and intermediates and the processes involved in ion formation and occurrence after 1064 nm laser irradiation, herein, we present some of our experimental results of HMX by using time-of-flight mass spectroscopy (TOFMS). A pulse

Address correspondence and reprint requests to: W. Zhang, Department of Applied Chemistry, School of Chemical Engineering, Nanjing University of Science and Technology, Nanjing, People's Republic of China. E-mail: wzhang@njust.edu.cn

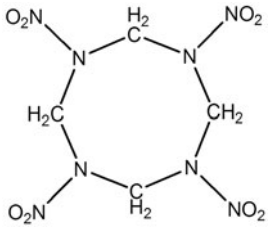

Fig. 1. Typical molecular structure of HMX.

laser at 1064 nm was used to ablate the solid HMX sample, mass spectra of both the negative and positive ions were recorded.

2. EXPERIMENTAL SECTION

The schematic of homemade reflection TOFMS has been given in previous publication (Zhang *et al*., 2013). The ablation was produced by a Nd:YAG solid-state laser source (LOTIS TII, LS-2147, Belarus) delivering pulses of 15 ns with energy up to 800 mJ at the wavelength of 1064 nm. The laser beam was focused onto the sample surface by using a focus lens. The HMX sample (about 50 mg) was compressed in a small aluminum cylindrical cup with 80 MPa pressure. The spectrometer consists of three basic regions: The ion source (also known as the extraction/acceleration region), the flight tube (also known as the field-free, or drift region), reflector, and the detector. The ion source is the region where ions are either introduced to the spectrometer or created. The flight tube is the region where ions are directed toward the detector and, most importantly, where mass separation takes place. Ions are accelerated out of the ion source towards the flight tube. The detector is a pair of microchannel plates (MCPs). The ions entering the extraction field were accelerated and travelled into the field-free tube, after being reflected by the reflector, these ions were finally detected by MCPs. A digital storage oscilloscope synchronized with the laser pulse and the TOFMS system recorded the collected mass spectra. Irradiation of the sample was performed in a vacuum chamber at a pressure of about 4×10^{-4} Pa. Laser energy was measured with an energy meter (Ophir, Model 30A, Israel).

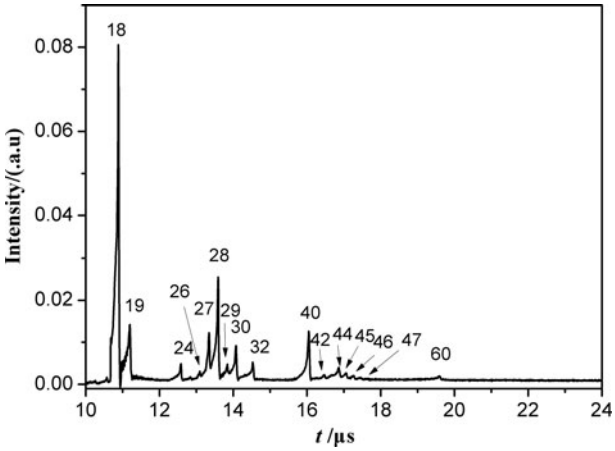

Fig. 3. Typical TOF mass spectrum of positive ions for HMX produced by 1064 nm laser ablation.

3. RESULTS AND DISCUSSION

For the negative ions (Fig. 2), three strong peaks appear at mass charge ratio (m/z) of 46, 60, and 106, according to the molecular structure and decomposition characteristics of HMX, these ions can be corresponded to NO_2, CH_2NO_2/N_2O_2, and $N(NO_2)_2/CH_2(NO_2)_2$, respectively. It may be pointed out that CH_2NO_2/N_2O_2, as well as $N(NO_2)_2/CH_2(NO_2)_2$, cannot be clearly distinguished due to the limited mass resolution of the spectrometer. This limited mass resolution is caused mainly by the large broadening of the kinetic energy distributions of the species produced in the ablation process. A relative strong peak at $m/z = 26$ can be ascribed to CN. Some other peaks can be seen at $m/z = 17, 30, 42$, 52, 88, 134, and 184, which may be due to OH, NO/CH_2O,

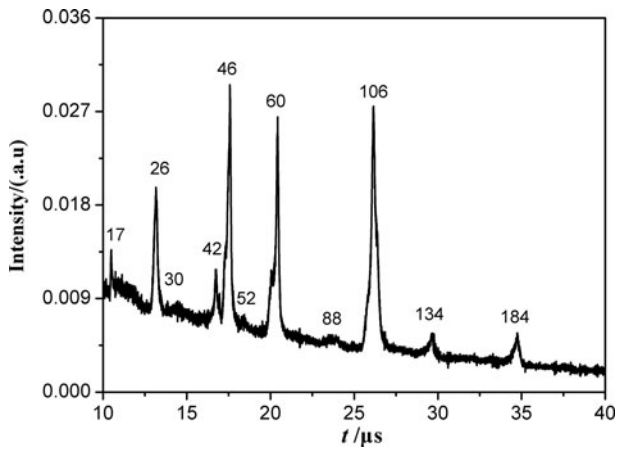

Fig. 2. Typical TOF mass spectrum of negative ions for HMX produced by 1064 nm laser ablation.

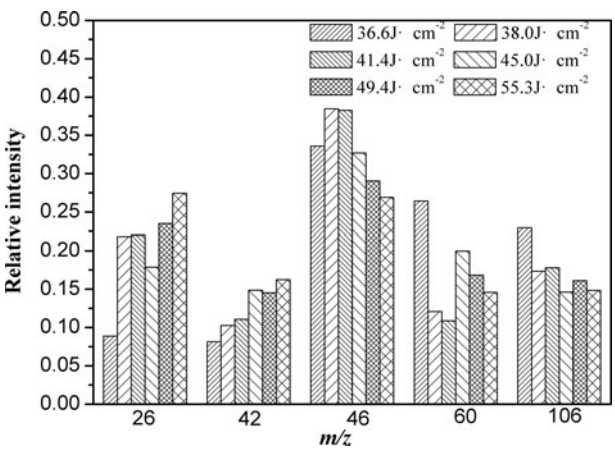

Fig. 4. Relative intensity of negative ions for HMX as a function of the laser fluence.

https://doi.org/10.1017/S0263034617000325 Published online by Cambridge University Press

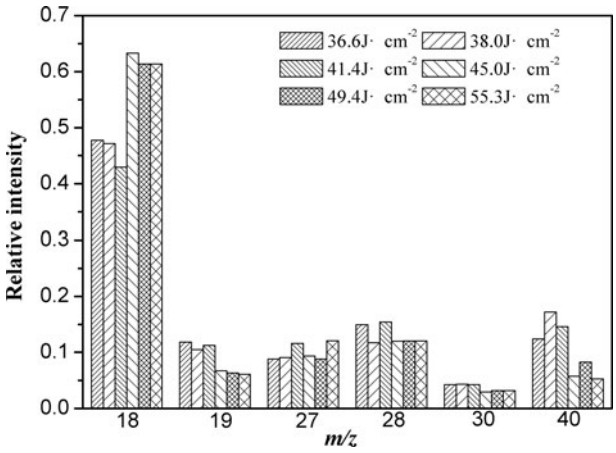

Fig. 5. Relative intensity of positive ions for HMX as a function of the laser fluence.

$CH_2N_2/C_2H_2O/CNO$, C_2N_2, $(CH_2)_2NNO_2$, $CH_2(NNO_2)_2$, and $CNN(CNNO_2)_2$, respectively.

From the TOF mass spectrum of the positive ions (Fig. 3), it can be noticed that three series of peaks are recorded. The first series are observed at $m/z = 18$ and 19, corresponding to H_2O and H_3O. The second series appear at $m/z = 24$, 26, 27, 28, 29, 30, and 32, possible assignments for these peaks are C_2, CN, HCN, $CO/N_2/H_2CN$, HCO, NO/CH_2O and O_2, respectively. Peaks at m/z values of 40, 42, 44, 45, 46, and 47 can be ascribed to CN_2/C_2H_2N, $CH_2N_2/C_2H_2O/CNO$, $N_2O/CO_2/CH_2NO$, HN_2O, NO_2, and HONO ions, respectively. Compared with our previous research, the mass spectra of HMX have certain similarities to that of cyclotrimethylenetrinitramine (RDX), this may be due to the similar molecular structure between RDX and HMX (Zhang *et al.*, 2014).

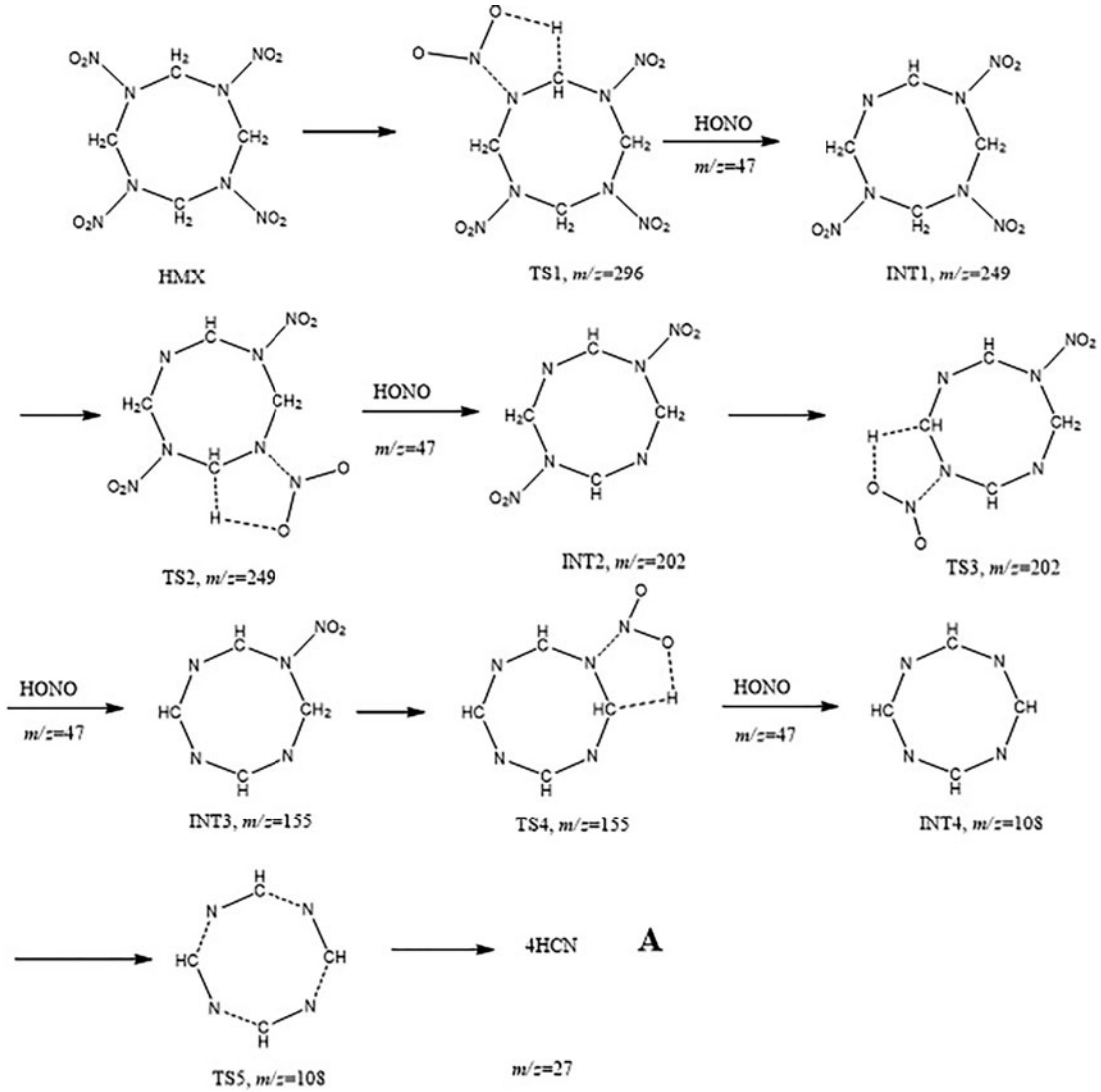

Fig. 6. Laser-induced HONO elimination pathways of HMX.

https://doi.org/10.1017/S0263034617000325 Published online by Cambridge University Press

By varying the laser fluence, the energy dependence of the relative intensity for the primary atom lines was obtained, as shown in Figures 4 and 5. For the negative ions (Fig. 4), with the increasing of the laser fluence, the relative intensity of $m/z =$ 42 gradually increased. Otherwise, the intensity of $m/z = 106$ showed the opposite tendency. The $m/z = 42$ particles perhaps produced by decomposing of $m/z = 106$. Moreover, the relative intensities of $m/z = 26$ and $m/z = 60$ also displayed an opposite tendency with the increasing of laser fluence, which indicated that CN may be product of CH_2NO_2 by losing two OH particles. The majority of particles lied in $m/z = 46$ under our experimental conditions, the relative intensity increased first and then decreased with the variation of laser fluence.

For the positive ions (Fig. 5), it was observed that the major positive ions appeared at $m/z = 18$ in the experimental fluence range, the relative intensity slightly decreased first, while the laser fluence was above 41.4 J/cm^2; the proportion increased sharply, above 50% of the positive ions are H_2O. The other positive ions could be found at $m/z = 19$, 27, 28, 30, and 40, the percentage of these ionic particles was under 15%. Most of the positive ions are not stable, they are easy to obtain the electron and change into neutral particles or negative ions.

According to the molecular structure, the main particles obtained by laser ablation of HMX can be considered to arise from three processes: HONO elimination, rupture of the N–NO_2 bond, and concerted symmetric ring fission of

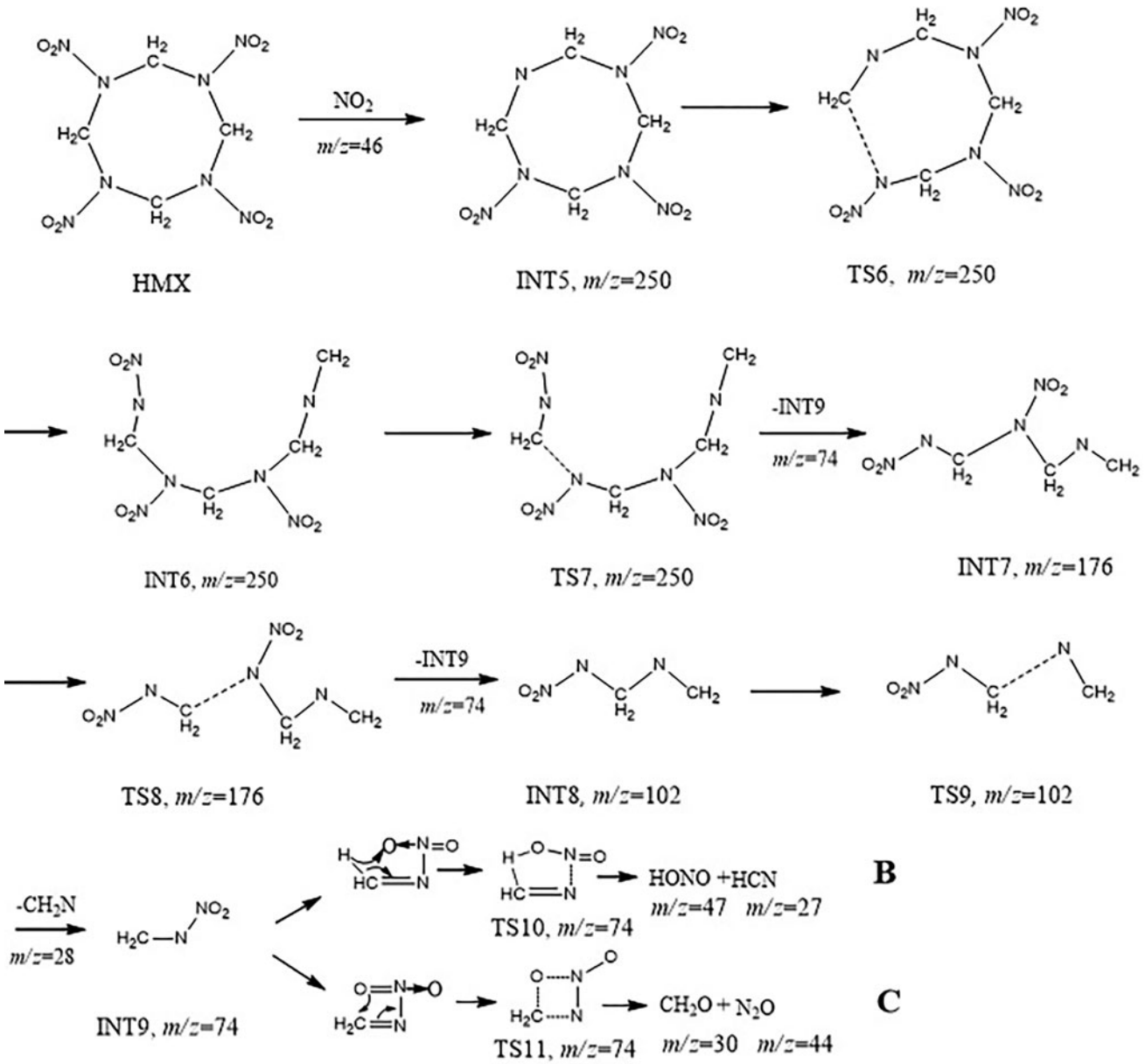

Fig. 7. Laser-induced rupture of the N–NO_2 bond pathways of HMX.

https://doi.org/10.1017/S0263034617000325 Published online by Cambridge University Press

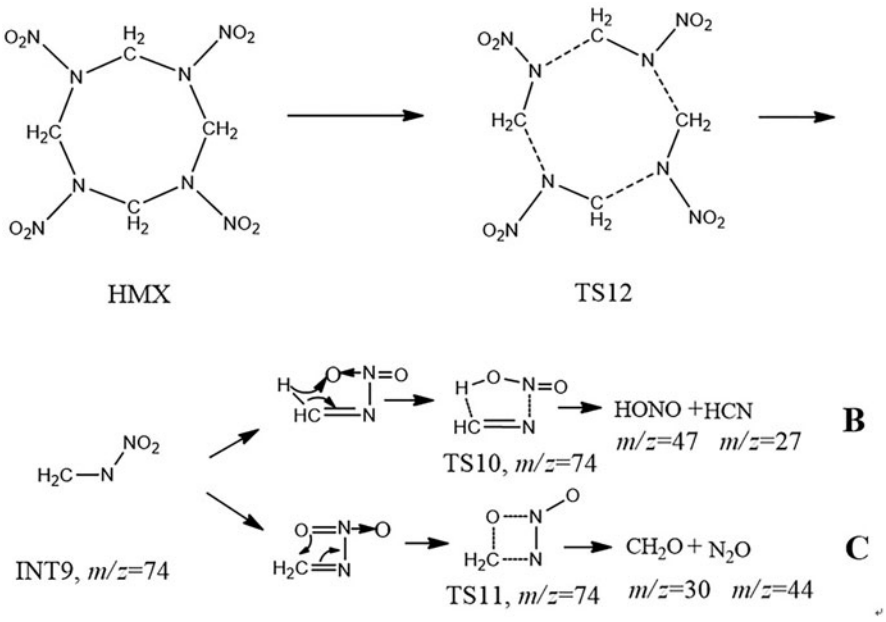

Fig. 8. Laser-induced concerted symmetric ring fission pathways of HMX.

HMX into four $CH_2N_2O_2$. The possible steps were proposed on the basis of TOFMS results and the structure of HMX, which were similar to the initial steps of theoretical calculation results (Lewis *et al.*, 2000).

Figure 6 shows laser-induced HONO elimination pathways of HMX. HONO particles were produced through cleavage of C–H bond of the ring and the adjacent N–N bond. N–N bond of HMX molecule was gradually stretched, and a hydrogen atom of its adjacent CH_2 got close to the oxygen atom of the nitro group, then transition state TS1 was formed, followed by the fracture of N–N and C–H bond, intermediate INT1 was produced by removing of a HONO ($m/z = 47$) fragment. The remaining nitro groups of INT1 would continue to experience a similar reaction to eliminate three HONO particles to generate intermediate INT4. Four C–N bonds of INT4 ring gradually extended to generate the transition state TS5, HCN ($m/z = 27$) particles were formed by cleavage of C–N bonds.

Figure 7 is laser-induced rupture of the N–NO_2 bond pathways of HMX. Possible peak assignments, together with a mechanism of formation of small particles, were proposed as: Loss of a nitro group ($m/z = 46$) from HMX molecular led to intermediate INT5, through a subsequent elongation of C–N bond, intermediate INT6 was formed via transition state TS6. This intermediate chain gave fragment INT7 at $m/z = 176$ via elimination of intermediate INT9 though transition state TS7. Thus, the same fragmentation process led to intermediate INT8 at $m/z = 102$ producing by transition state TS8. INT7 arose from transition state TS9 through loss of CH_2N fragment. INT9 could generate smaller particles through two different paths, HONO ($m/z = 47$) and HCN ($m/z = 27$) could be generated via the transition state TS10 (Path B), CH_2O ($m/z = 30$) and N_2O ($m/z = 44$) could also be generated via transition state TS11 (path C).

Another possible laser-induced decomposition pathway is shown in Figure 8. The four non-adjacent C–N bonds on the eight-membered ring were gradually elongated to form the transition state TS12, followed by the simultaneous fracture of the C-N bonds, INT9 was produced, INT9 might undergo the similar reaction with the reaction shown in Figure 7 to form HONO, HCN, CH_2O, and N_2O.

4. CONCLUSIONS

We have presented an experimental investigation of the ions produced during 1064 nm laser ablation of HMX in vacuum by TOF mass spectrometry. Important negative and positive ions were observed, consisting of mostly low-molecular-mass species. Most of these products resulted mainly from HONO elimination, N–NO_2 bond breaking, and concerted symmetric ring fission pathways. Some other reactions may exist to account for the undetermined ions hence, it is necessary to develop other experimental and theoretical methods to confirm the process of these reactions, which will help to understand the laser initiation of HMX.

ACKNOWLEDGMENTS

This work was supported by the National Natural Science Foundation of China (No. 11604149) and a Project Funded by the Priority Academic Program Development of Jiangsu Higher Education Institutions (PAPD).

REFERENCES

Abdulazeem, M., Alhasan, A. & Abdulrahmann, S. (2011). Initiation of solid explosives by laser. *Int. J. Therm. Sci.* **50**, 2117–2121.

https://doi.org/10.1017/S0263034617000325 Published online by Cambridge University Press

Ahmad, S.R., Russell, D.A. & Golding, P. (2009). Laser-induced deflagration of unconfined HMX–the effect of energetic binders. *Propell., Explos., Pyrot.* **34**, 513–519.

Ali, A., Son, S., Asay, B., Decroix, M. & Brewster, M. (2003). High-irradiance laser ignition of explosives. *Combust. Sci. Technol.* **175**, 1551–1571.

Aluker, E., Aluker, N., Krechetov, A., Mitrofanov, A.Y., Nurmukhametov, D. & Shvaiko, V. (2011). Laser initiation of PETN in the mode of resonance photoinitiation. *Russ. J. Phys. Chem. B.* **5**, 67–74.

Aluker, E., Belokurov, G., Krechetov, A., Mitrofanov, A.Y. & Nurmukhametov, D. (2010). Laser initiation of PETN containing light-scattering additives. *Tech. Phys. Lett.* **36**, 285–287.

Aluker, E.D., Krechetov, A.G., Mitrofanov, A.Y., Zverev, A.S. & Kuklja, M.M. (2012). Understanding limits of the thermal mechanism of laser initiation of energetic materials. *J. Phys. Chem. C.* **116**, 24482–24486.

Babushok, V., DeLucia, F., Dagdigian, P., Gottfried, J., Munson, C., Nusca, M. & Miziolek, A. (2007). Kinetic modeling study of the laser-induced plasma plume of cyclotrimethylenetrinitramine (RDX). *Spectrochim. Acta B.* **62**, 1321–1328.

Bhattacharya, A., Guo, Y. & Bernstein, E.R. (2010). Nonadiabatic reaction of energetic molecules. *Accounts Chem. Res.* **43**, 1476–1485.

Bhattacharya, A., Guo, Y. & Bernstein, E.R. (2012). A comparison of the decomposition of electronically excited nitro-containing molecules with energetic moieties C-NO_2, N-NO_2, and O-NO_2. *J. Chem. Phys.* **136**, 024321.

Bourne, N. (2001). On the laser ignition and initiation of explosives. *Proc. R. Soc. Lond. A* **457**, 1401–1426.

Civiš, M., Civiš, S., Sovová, K.N., Dryahina, K., Španěl, P. & Kyncl, M. (2011). Laser ablation of FOX-7: Proposed mechanism of decomposition. *Anal. Chem.* **83**, 1069–1077.

Cohen, R., Zeiri, Y., Wurzberg, E. & Kosloff, R. (2007). Mechanism of thermal unimolecular decomposition of TNT (2, 4, 6-trinitrotoluene): A DFT study. *J. Phys. Chem. A* **111**, 11074–11083.

Damm, D. & Maiorov, M. (2010). Thermal and radiative transport analysis of laser ignition of energetic materials. *Proc. SPIE* **7795**, 779502–779512.

Dik, I.G., Sazhenova, E.A. & Selikhovkin, A.M. (1991). A role of gas phase on transition into combustion of a condensed matter by radiation stream ignition. *Fizika Goreniya I Vzryva* **27**, 7–12.

Greenfield, M., Guo, Y. & Bernstein, E. (2006). Ultrafast photodissociation dynamics of HMX and RDX from their excited electronic states via femtosecond laser pump–probe techniques. *Chem. Phys. Lett.* **430**, 277–281.

Kuklja, M. (2003). On the initiation of chemical reactions by electronic excitations in molecular solids. *Appl. Phys. A.* **76**, 359–366.

Kuklja, M.M., Aduev, B., Aluker, E., Krasheninin, V., Krechetov, A. & Mitrofanov, A.Y. (2001). Role of electronic excitations in explosive decomposition of solids. *J. Appl. Phys.* **89**, 4156–4166.

Lee, K.-C., Kim, K.-H. & Yoh, J.J. (2008). Modeling of high energy laser ignition of energetic materials. *J. Appl. Phys.* **103**, 083536.

Lewis, J.P., Glaesemann, K.R., VanOpdorp, K. & Voth, G.A. (2000). Ab initio calculations of reactive pathways for α-Octahydro-1,3,5,7-tetranitro-1,3,5,7-tetrazocine (α-HMX). *J. Phys. Chem. A.* **104**, 11384–11389.

Meredith, K.V., Gross, M.L. & Beckstead, M.W. (2015). Laser-induced ignition modeling of HMX. *Combust. Flame* **162**, 506–515.

Myers, T.W., Bjorgaard, J.A., Brown, K.E., Chavez, D.E., Hanson, S.K., Scharff, R.J., Tretiak, S. & Veauthier, J.M. (2016). Energetic chromophores: Low-energy laser initiation in explosive Fe(II) tetrazine complexes. *J. Am. Chem. Soc.* **138**, 4685–4692.

Pravica, M., Galley, M., Kim, E., Weck, P. & Liu, Z. (2010). A far- and mid-infrared study of HMX (octahydro-1,3,5,7-tetranitro-1,3,5,7-tetrazocine) under high pressure. *Chem. Phys. Lett.* **500**, 28–34.

Sharia, O., Tsyshevsky, R. & Kuklja, M.M. (2013). Surface-accelerated decomposition of δ-HMX. *J. Phys. Chem. Lett.* **4**, 730–734.

Shui, M., Sun, Y., Zhao, Z., Cheng, K., Xiong, Y., Wu, Y., Fan, W., Yu, J., Yan, Y., Yang, Z., Gu, Y., Zhong, F. & Xu, T. (2013). Photothermal decomposition of HNS at 532 nm. *Optik.* **124**, 6115–6118.

Sunku, S., Gundawar, M.K., Myakalwar, A.K., Kiran, P.P., Tewari, S.P. & Rao, S.V. (2013). Femtosecond and nanosecond laser induced breakdown spectroscopic studies of NTO, HMX, and RDX. *Spectrochim. Acta B* **79**, 31–38.

Tang, C.-J., Lee, Y.J., Kudva, G. & Litzinger, T.A. (1999). A study of the gas-phase chemical structure during CO_2 laser assisted combustion of HMX. *Combust. Flame.* **117**, 170–188.

Wang, F., Tsyshevsky, R.V., Zverev, A.S., Mitrofanov, A.Y. & Kuklja, M.M. (2017). Can a photo-sensitive oxide catalyze decomposition of energetic materials? *J. Phys. Chem. C* **121**, 1153–1161.

Yazdani, E., Cang, Y., Sadighi-Bonabi, R., Hora, H. & Osman, F. (2009). Layers from initial Rayleigh density profiles by directed nonlinear force driven plasma blocks for alternative fast ignition. *Laser Part. Beams* **27**, 149–156.

Zhang, W., Shen, R., Wu, L., Ye, Y., Hu, Y. & Zhu, P. (2013). The formation mechanism of clusters produced by laser ablation of solid sodium azide. *Laser Phys. Lett.* **10**, 026002.

Zhang, W., Shen, R., Ye, Y., Wu, L., Hu, Y. & Zhu, P. (2014). Dissociation of Cyclotrimethylenetrinitramine Under 1064-nm Laser Irradiation Investigated by Time-of-Flight Mass Spectrometer. *Spectrosc. Lett.* **47**, 611–615.

Zhang, W., Shen, R., Ye, Y., Wu, L., Hu, Y. & Zhu, P. (2015). Photodissociation of 2, 4, 6-trinitrotoluene with a Nd: YAG laser at 532 nm. *Proc. SPIE* **9543**, 9543A.

https://doi.org/10.1017/S0263034617000325 Published online by Cambridge University Press